Biomaterials xxx (2011) 1–12

Contents lists available at ScienceDirect

Biomaterials

journal homepage: www.elsevier.com/locate/biomaterials

Tunable physiologic interactions of adhesion molecules for inflamed cell-selective drug delivery

Sungkwon Kang [a], Taehyun Park [a], Xiaoyue Chen [a], Greg Dickens [a], Brian Lee [a], Kevin Lu [a], Nikolai Rakhilin [a], Susan Daniel [b], Moonsoo M. Jin [a,*]

[a] Department of Biomedical Engineering, Cornell University, Ithaca, NY 14853, USA
[b] Department of Chemical and Biomolecular Engineering, Cornell University, Ithaca, NY 14853, USA

ARTICLE INFO

Article history:
Received 19 December 2010
Accepted 6 January 2011
Available online xxx

Keywords:
Integrin
ICAM-1
Avidity
Celastrol
Inflammation
Drug delivery

ABSTRACT

Dysregulated inflammation contributes to the pathogenesis of various diseases. Therapeutic efficacy of anti-inflammatory agents, however, falls short against resilient inflammatory responses, whereas long-term and high-dose systemic administration can cause adverse side effects. Site-directed drug delivery systems would thus render more effective and safer treatments by increasing local dosage and minimizing toxicity. Nonetheless, achieving clinically effective targeted delivery to inflammatory sites has been difficult due to diverse cellular players involved in immunity and endogenous targets being expressed at basal levels. Here we exploit a physiological molecular interaction between intercellular adhesion molecule (ICAM)-1 and lymphocyte function associated antigen (LFA)-1 to deliver a potent anti-inflammatory drug, celastrol, specifically and comprehensively to inflamed cells. We found that affinity and avidity adjusted inserted (I) domain, the major binding site of LFA-1, on liposome surface enhanced the specificity toward lipopolysaccharides (LPS)-treated or inflamed endothelial cells (HMEC-1) and monocytes (THP-1) via ICAM-1 overexpression, reflecting inherent affinity and avidity modulation of these molecules in physiology. Targeted delivery of celastrol protected cells from recurring LPS challenges, suppressing pro-inflammatory responses and inflammation-induced cell proliferation. Targeted delivery also blocked THP-1 adhesion to inflamed HMEC-1, forming barriers to immune cell accumulation and to aggravating inflammatory signals. Our results demonstrate affinity and avidity of targeting moieties on nanoparticles as important design parameters to ensure specificity and avoid toxicities. We anticipate that such tunable physiologic interactions could be used for designing effective drug carriers for *in vivo* applications and contribute to treating a range of immune and inflammatory diseases.

1. Introduction

Imbalance between pro- and anti-inflammatory responses of host immune system contributes to the pathogenesis of various human diseases of modern society [1]. In particular, prolonged and excessive inflammation, which comprises persistently reinitiating acute and chronic inflammatory responses between non-immune (epithelium, endothelium, etc) and immune cells, has been implicated in cardiovascular diseases [2], obesity [3], neurodegenerative diseases [4], and cancer [5]. Subsequently, anti-inflammatory agents such as corticosteroids, nonsteroidal anti-inflammatory drugs, cyclo-oxygenase-2-selective inhibitors, and statins have been used clinically to treat acute and chronic inflammatory diseases [6–9]. Long-term and high-dose enteral or parenteral administration of these drugs, however, have been limited due to adverse systemic side effects that included gastrointestinal disturbances, renal, ocular and liver toxicities, skeletal and muscle damages, and increased risk of cardiovascular diseases [10–13].

Current advances in site-directed drug delivery systems [14] would thus contribute much benefit towards safer and more effective clinical use of anti-inflammatory agents. Numerous studies have targeted drug carriers to the endogenous molecules of endothelium such as ICAM-1 [15,16], vascular cell adhesion molecule (VCAM)-1 [17,18], platelet endothelial cell adhesion molecule (PECAM)-1 [19], E- and P-selectins [20,21], and $\alpha_v\beta_3$ integrin [22,23], which belong to a family of cell adhesion molecules. Some of the cell adhesion molecules such as E-selectins and $\alpha_v\beta_3$ integrin are more exclusively expressed in vascular endothelium, while others may be present in both non-immune and immune cells. The difference in their response to inflammation is also observed in terms of the levels of

* Corresponding author. Fax: +1 607 255 7330.
E-mail address: mj227@cornell.edu (M.M. Jin).

0142-9612/$ – see front matter © 2011 Elsevier Ltd. All rights reserved.
doi:10.1016/j.biomaterials.2011.01.046

induction as well as their basal expression prior to inflammation. ICAM-1 has been of particular interest for its superior inducible and localized expression upon inflammatory stimuli both in immune and non-immune cells such as endothelial, smooth muscle, epithelial cells, fibroblasts, lymphocytes, and myeloid cells [24,25]. Specific delivery of drug carriers or nanoparticles to inflamed cells has traditionally been achieved by molecular interactions with cell surface molecules created by attaching antibodies or short peptides to the surface of nanoparticles [26,27]. However, most prior approaches have failed to address affinity and avidity modulation as important design criteria for efficient nanoparticle binding to target cells, which will be drastically different from those for free molecule binding due to much larger detachment force on nanoparticles caused by hydrodynamic stress *in vitro* and *in vivo*. Alternative to non-native interactions, the use of physiological ligands or their engineered variants [28–30] conjugated to nanoparticles at an optimal density for tunable affinity and avidity may prove advantageous in regard to ensuring specificity against target receptors and a lower risk of unwanted immune response.

In any attempt to deliver drugs via ICAM-1 targeting, one needs to ensure specific delivery of drug carriers to inflamed cells but not to normal cells, given the observation that ICAM-1 is broadly expressed in the body albeit at much lower levels than post exposure to inflammatory stimuli [31]. In order to design drug carriers against ICAM-1 to be robust and amenable to fine-control in terms of affinity and avidity, we have chosen a targeting moiety based on a native molecule called the inserted or I domain, derived from a physiological receptor to ICAM-1 called lymphocyte function associated antigen (LFA)-1 integrin [25,28]. In contrast to commonly used monoclonal antibodies (~150 kDa) against ICAM-1 for targeting, LFA-1 I domain is small (~20 kDa) and suitable for a low-cost, large-scale production in bacteria, and can be modified for optimal affinity to ICAM-1 and facile conjugation to drug carriers. Among various nanoparticles suitable for drug delivery, liposomes have been used in this study, which have been approved for clinical use to take advantage of diverse functionalized phospholipids and large compartments for encapsulation of both hydrophilic and hydrophobic molecules. To the surface of liposomes, high affinity LFA-1 I domain (Id-HA) was attached via non-covalent, His-tag binding to nickel ions chelated onto phospholipid molecules. As a model anti-inflammation drug, we incorporated celastrol, a quinone methide triterpene, into the liposomes. Celastrol possesses potent anti-inflammatory, anti-oxidative, and anti-proliferative activities via the inhibition of NF-κB signaling and proteasome activity [32–34].

In this study, we emphasized the delivery of celastrol selectively to inflamed cells without causing cytotoxicity while maintaining potent therapeutic effect. To implement this, the density of Id-HA on the surface of liposomes was adjusted for optimal dose and specificity. We then examined whether such targeted delivery conditions could elicit the anti-inflammatory effect of celastrol in inflamed endothelium and myeloid cells in a manner dependent on ICAM-1 and LFA-1 interaction. As for the measure of selective delivery of celastrol, we investigated its ability to inhibit gene and protein expression of pro-inflammatory mediators and to block the migration of monocytes, which together may form a key barrier to immune cell accumulation and to aggravating inflammatory responses in physiology.

2. Materials and methods

2.1. Cell culture

Human dermal microvascular endothelial cells (HMEC-1) were obtained from the Center for Disease Control. HMEC-1 were cultured in MCDB 131 medium (Invitrogen) supplemented with 10% FBS (Atlanta Biologicals), 10 mM L-glutamine, Pen-strep (100 units/ml penicillin and 100 μg/ml streptomycin), 1 μg/ml hydrocortisone (MP Biomedicals), and 10 ng/ml recombinant human epidermal growth factor (Invitrogen). HMEC-1 were trypsinized when confluent, and gently centrifuged and washed to remove residual trypsin before plating. Human monocytic leukemia THP-1 cells (ATCC) were grown in RPMI 1640 medium (Invitrogen) with 10% FBS and Pen-strep. HeLa cells were propagated in Advanced DMEM medium (Invitrogen) containing 10% FBS and 2 mM L-glutamine, and Pen-strep. Mouse brain microvascular endothelial cells (bEnd.3, ATCC) were maintained in Advanced DMEM medium supplemented with 4 mM L-glutamine, Pen-strep, and 10% FBS. For induction of inflammation, HMEC-1, THP-1, or bEnd.3 cells were treated with 1 μg/ml of LPS (*Escherichia coli*. 026:B6, Sigma). All mammalian cells were maintained at 37 °C in a 5% CO_2 humidified incubator.

2.2. Production of I domains and GFP-Id-HA fusion protein

The wild-type (WT), D137A, and F265S/F292G mutants of LFA-1 I domains (Id-WT, Id-D137A, and Id-HA) were produced as previously described [28,30]. Briefly, the I domains (Asn129 to Tyr307) followed by a stop codon were subcloned into pET28a vector (Novagen) between NheI and XhoI for expression with a His-tag at the N-terminal. The I domains were expressed in *E. coli* BL21 (DE3) cells (Novagen) as inclusion bodies. Cells were initially grown to OD600 of 0.4–0.5 and induced with 1 mM IPTG (isopropyl-β-D-thiogalactoside) for 6 h at 37 °C. To isolate the inclusion bodies, cells were resuspended in washing buffer (50 mM Tris-Cl (pH 8.0), 23% (w/v) sucrose, 1 mM EDTA, 0.5% (v/v) Triton X-100) and sonicated. Inclusion bodies were washed by repeating cycles of centrifugation, removal of supernatant, and sonication until pure pellets were obtained. Inclusion bodies were then solubilized in denaturing buffer (50 mM Tris-Cl (pH 8.0), 6 M guanidine HCl) and diluted in refolding buffer (50 mM Tris-Cl (pH 8.0), 15% glycerol, 1 mM $MgCl_2$) to a volume such that the final concentration of guanidine HCl was less than 25 mM. Refolded proteins were concentrated and subjected to gel filtration chromatography using Superdex S200 column in HBS (20 mM HEPES, 140 mM NaCl, pH 7.4) connected to AKTA Purifier (GE Healthcare). Some of the I domains were conjugated to Alexa Fluor 488 (AF488, Invitrogen) according to the instruction of the vendor. For GFP-Id-HA fusion protein, eGFP (Val2 to Lys239) [35] was first inserted into pET28a vector between NheI and BamHI and then Id-HA (Asn129 to Tyr307) followed by a stop codon was placed between BamHI and XhoI. GFP-Id-HA was produced from soluble fractions in BL21 cells. Cells were grown to OD600 of 0.4–0.5, induced with 1 mM IPTG at 25 °C for 6 h and recovered by centrifugation. Cells were then resuspended and sonicated in NTA (nitrilotriacetic acid) binding buffer (50 mM NaH_2PO_4 (pH 8.0), 300 mM NaCl, 10 mM imidazole). Soluble proteins were separated from cell debris by centrifugation, purified by flowing the supernatant through a Ni-NTA column (Novagen) and gel filtration chromatography using S200 column.

2.3. Immunofluorescence flow cytometry and microscopy

Antibodies used for this study include anti-ICAM-1 monoclonal antibody (mAb) LB-2 (Santa Cruz) and anti-VCAM-1 mAb P3C4 (Developmental Studies Hybridoma Bank). If necessary, phycoerythrin (PE)-labeled goat anti-mouse IgG (Santa Cruz) was used for the detection of primary mAbs. For flow cytometric analysis (Beckman Coulter EPICS XL-MC), cells were trypsinized, washed with ice-chilled labeling buffer (PBS (pH 7.4), 0.5% (w/v) BSA, 10 mM $MgCl_2$), and incubated on ice for 20 min. Antibodies and proteins were used at 10 μg/ml in 200 μl of the labeling buffer and were incubated with cells on ice for 30 min. Cells were washed twice in 500 μl of the labeling buffer between each step of labeling when secondary antibodies were needed. After final washing, cells were resuspended in 300 μl of the labeling buffer and subjected to flow cytometer. For immunofluorescence microscopy, HMEC-1 were fixed with 3.7% paraformaldehyde for 30 min, washed and labeled with mAbs LB-2 or P3C4 in labeling buffer (PBS, 1% BSA, 0.02% (v/v) Tween 20) on a rocker at room temperature for 2 h. DAPI (4′,6-diamidino-2-phenylindole, Invitrogen) was used at 300 nM in PBS for 10 min for nucleus staining. To estimate fluorescence and nuclei density from DAPI staining, microscopic images of 4 random spots were acquired and processed by Image-Pro Plus (Media Cybernetics) for automated intensity measurement and object counting. Similarly, confluent bEnd.3 cells were incubated with AF488 conjugated Id-HA. Stained cells were washed and imaged with a fluorescence microscope (Zeiss Axio Observer Z1). For confocal microscopy (Leica TCS SP2), HeLa cells were labeled with 10 μg/ml of mAb LB-2 or GFP-Id-HA in 200 μl of labeling buffer on ice for 30 min.

2.4. LFA-1 or Mac-1 I domain-displaying yeast binding to HMEC-1

Mammalian cell surface binding of yeast cells displaying various I domains was performed as previously described [35]. In short, yeast cells expressing WT or activated mutants of LFA-1 and Mac-1 I domains were washed and resuspended in washing buffer (PBS (pH 7.4), 0.5% BSA, 10 mM $MgCl_2$). 300 μl of yeast cell suspension containing approximately 5×10^7 cells was applied to each well of confluent HMEC-1 in a 24-well plate. Yeast cells were allowed to bind to HMEC-1 for 1 h at room temperature. Cells were then washed with washing buffer by gentle shaking on an orbital shaker for 15 min.

Please cite this article in press as: Kang S, et al., Tunable physiologic interactions of adhesion molecules for inflamed cell-selective drug delivery, Biomaterials (2011), doi:10.1016/j.biomaterials.2011.01.046

2.5. Preparation of I domain coupled liposomes

Liposomes were prepared by the thin lipid film method followed by the sonication and extrusion method [36]. Phospholipid (Avanti Polar Lipids) mixture was prepared by mixing 52.5 mol % DPPC (1,2-dipalmitoyl-*sn*-glycero-3-phosphocholine), 12.5 mol % DPPE (1,2-dipalmitoyl-*sn*-glycero-3-phosphoethanolamine), 20 mol % cholesterol, 5 mol % PEG1000-PE (1,2-dimyristoyl-*sn*-glycero-3-phosphoethanolamine-N-[methoxy(polyethylene glycol)-1000]), and 10 mol% DOGS-NTA(Ni) (1,2-dioleoyl-*sn*-glycero-3-[(N-(5-amino-1-carboxypentyl)iminodiacetic acid)succinyl]) in chloroform. Chloroform in the lipid mixture in a round bottom flask was then evaporated with nitrogen gas to form a lipid film. Lipid films were rehydrated with HBS (20 mM HEPES, 140 mM NaCl, pH 7.4) containing 10 mM FITC (fluorescein isothiocyanate) or 1 mM celastrol. Rehydrated multilamellar vesicular liposomes were then sonicated (Misonix Sonicator 3000) and extruded 10 times through 100 nm polycarbonate membranes (Nuclepore, Whatman). Extruded unilamellar vesicular liposomes were supplemented with 10 mM $NiCl_2$ and collected by centrifugation at 35,000 rpm for 2 h. Supernatant was removed, leaving a final volume of approximately 500 μl. Pelleted liposomes were gently sonicated (Branson Sonified 150), filtered through 0.2 μm centrifugal filters, and subjected to S200 column (GE Healthcare) in HBS. Liposome diameters were measured using dynamic light scattering (Zetasizer Nano-S, Malvern Instruments). Encapsulation efficiency of FITC was estimated by fluorescence (excitation 490 nm/emission 520 nm) and celastrol by absorbance at 425 nm (extinction coefficient, 10,063 M^{-1} cm^{-1}) after lipid solubilization with 1% (v/v) Triton X-100. Liposomes encapsulating FITC or celastrol were mixed with I domains and incubated on ice for 30 min for spontaneous coupling. For all couplings, a mass ratio of I domains to liposomes was 20% unless otherwise stated. Coupling efficiency of His-tagged I domains to liposomes was estimated by sucrose gradient flotation assay. Liposome/I domain mixture was diluted to final 30% (w/v) sucrose, layered with 20% sucrose solution, and centrifuged at 35,000 rpm for 2 h. After centrifugation, top fractions were collected and estimated for protein concentrations by Lowry method (Bio-Rad DC Protein Assay Kit).

2.6. Liposome delivery into endothelium and monocytes

HMEC-1 or THP-1 cells were initially grown to confluence in 24-well plates and treated with 1 μg/ml LPS for 24 h to induce inflammation. The liposome/I domain mixtures were adjusted to a final volume of 300 μl with prewarmed complete growth media containing 10% FBS and added to cells. HMEC-1 or THP-1 cells were treated with the preassembled liposomes or other control treatments at 37 °C for 30 min and washed twice with complete growth media. At 36–48 h after incubation, cells were challenged again with 1 μg/ml LPS for 3 h for quantitative PCR gene expression analysis or 24 h for THP-1 cell adhesion assay. For cell viability assays, HMEC-1 in 24-well plates were treated with basal media containing 0.5 mg/ml of MTT (3-(4,5-Dimethylthiazol-2-yl)-2,5-diphenyltetrazolium bromide) for 4 h at 37 °C. Blue formazan products were solubilized with DMSO and the absorbance was measured at 570 nm with a plate reader (Infinite M1000, TECAN).

2.7. Real-time quantitative RT-PCR

Total RNA was extracted using TRI Reagent (Ambion). Briefly, cells in 24-well plates were given 200 μl TRI Reagent for each well. Homogenized lysates were mixed with 40 μl of chloroform and centrifuged for 15 min at 12,000 x g. 80 μl of the colorless upper aqueous phase was carefully collected and mixed with 200 μl isopropanol. Samples were loaded to spin columns (Zymo-Spin II, Zymo Research) and washed twice with 500 μl ethanol. RNA was eluted with 30 μl of RNase-free water (UltraPure, Invitrogen). 500 ng of total RNA was reverse-transcribed at 25 °C for 10 min, 37 °C for 2 h, and 85 °C for 5 min using a reverse transcription kit (High Capacity cDNA RT Kits, Applied Biosystems) in a thermal cycler (GeneAmp PCR System 2700, Applied Biosystems). 2 μl of the cDNA product was used for real-time gene amplification analysis. Master mix 2X qPCR kit (Sybr Green 2x Master Mix, Bio-Rad) was used to amplify the specified genes for quantitative PCR (MyiQ iCycler, Bio-Rad). Gene expression was normalized to a house keeping gene ATP5J. Intron spanning primers were designed from the National Institute of Health qPrimerDepot using accession codes of NM_000201 (ICAM-1), NM_001078 (VCAM-1), NM_002982 (MCP-1), NM_000575 (IL-1α), NM_000594 (TNF-α), NM_000450 (E-selectin), NM_001250 (CD40) and NM_001003703 (ATP5J).

2.8. THP-1 cell adhesion assay

THP-1 cells were suspended at 10^6 cells/ml in complete growth media containing 10% FBS and labeled with 2 μg/ml BCECF-AM (2,7-bis-(2-carboxyethyl)-5-(and-6)-carboxyfluorescein acetoxymethyl ester, Invitrogen) for 30 min at 37 °C. BCECF-labeled THP-1 cells were washed and resuspended at 2 x 10^6 cells/ml in growth media. 300 μl of the THP-1 cell suspension was applied to each well of HMEC-1 in 24-well plates and allowed to bind for 30 min at 37 °C. Cells were repeatedly washed with complete growth media until THP-1 cells on resting HMEC-1 were cleared. THP-1 cells were then imaged by a fluorescence microscope and lysed with a lysis buffer (PBS (pH 7.4), 1% (v/v) Triton X-100) by vigorously shaking the plate for 1 h at room temperature. Fluorescence (excitation 490 nm/emission 535 nm) of the cell lysates was measured by a plate reader.

2.9. Statistical analysis

Data were expressed as mean ± standard deviation (S.D.) of at least quadruplicate samples. Statistical analysis of data was carried out using GraphPad Prism 5. Unpaired student's *t*-test was used to determine statistical significance in comparison to matching controls (Figs. 1 and 2). One-way ANOVA was used to compare mean responses among different liposome and control treatments (Figs. 6 and 7), followed by Tukey's post-hoc test to determine statistical significance.

3. Results

3.1. Detection of temporal upregulation of ICAM-1 in endothelium and monocytes

Upregulated expression of ICAM-1 is associated with almost all cellular players in acute and chronic inflammation [24]. Diversity of the cellular components and their complex inflammatory signaling network present a challenge to developing an effective anti-inflammatory therapy. We used HMEC-1 and THP-1 representing major non-immune and immune cells, respectively that constitute an inflammatory milieu. To induce inflammation, cells were treated with LPS that activate NF-κB dependent inflammatory signaling pathways [37]. In resting HMEC-1 and THP-1 cells, ICAM-1 expression was below the detection limit with anti-ICAM-1 mAb LB-2 (Fig. 1A). LPS treatment gradually induced ICAM-1 expression in both HMEC-1 and THP-1 cells, peaking at 12–24 h (Fig. 1A). We then tested whether a physiologic counter-receptor for ICAM-1, the I domain from human LFA-1 integrin containing two activating mutations (F265S/F292G) (abbreviated as Id-HA) [28,30], would detect a comparable temporal induction of ICAM-1. To measure Id-HA binding to ICAM-1 without any additional labels, Id-HA was expressed as a fusion to GFP (GFP-Id-HA) and tested for its binding to HeLa cells with constitutive expression of ICAM-1 (Fig. 1B). ICAM-1 staining with Id-HA in HeLa was comparable to mAb LB-2, shown by confocal microscopy (Fig. 1C). The temporal induction of ICAM-1 in HMEC-1 and THP-1 cells measured by flow cytometry using GFP-Id-HA was in good agreement with ICAM-1 staining with mAb LB-2 (Fig. 1E). We also found that human Id-HA cross-reacts with murine ICAM-1, confirmed with mouse brain microvascular endothelial cells (bEnd.3) after LPS treatment (Fig. 1D). Cross-reactivity of Id-HA with murine ICAM-1 will be of significant advantage as the identical formulation can be applied to both human cells and mouse models in preclinical studies.

3.2. Suppression of various pro-inflammatory mediators by celastrol

Celastrol is a plant derived quinone methide triterpene (Fig. 2A), long been known for potent anti-inflammatory, anti-oxidative, and anti-proliferative activities. Previous studies have shown celastrol as a potent antagonist of proteasomes and NF-κB signaling [32–34]. To examine whether celastrol can be used as a model drug for the suppression of inflammation in both HMEC-1 and THP-1 cells, we first assessed its inhibitory effect on LPS-induced gene expression of various pro-inflammatory mediators by quantitative real-time PCR (Fig. 2B and C). LPS treatment highly upregulated various cytokines, chemokines, and cell surface molecules in both HMEC-1 and THP-1 cells compared with their resting states (Fig. 2B and C). In HMEC-1, interleukin (IL)-1α, monocyte chemotactic protein (MCP)-1, CD40, E-selectin, ICAM-1, and VCAM-1 were greatly upregulated as early as 3 h treatment with LPS (Fig. 2B). Similarly in THP-1 cells, tumor necrosis factor (TNF)-α, MCP-1, ICAM-1, VCAM-1, and CD40 were highly upregulated (Fig. 2C). Relative fold inductions of ICAM-1 and

Please cite this article in press as: Kang S, et al., Tunable physiologic interactions of adhesion molecules for inflamed cell-selective drug delivery, Biomaterials (2011), doi:10.1016/j.biomaterials.2011.01.046

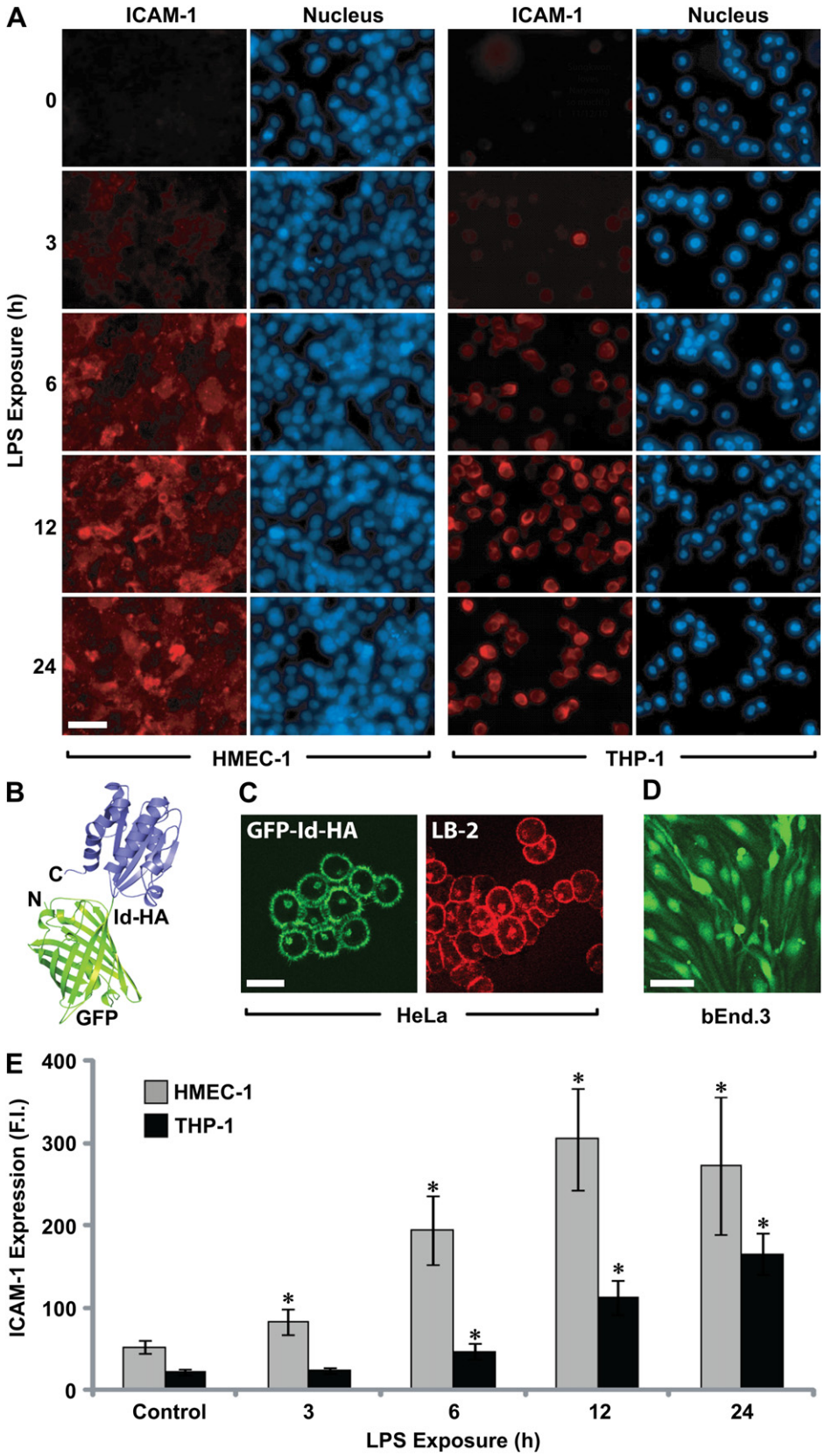

Fig. 1. Inflammation-induced upregulation of ICAM-1 in HMEC-1 and THP-1 cells. (A) Confluent HMEC-1 and THP-1 cells were exposed to LPS (1 μg/ml) for 0–24 h. ICAM-1 expression and nuclei were detected by immunofluorescence staining with mAb LB-2 and DAPI, respectively (scale bar, 50 μm). (B) A model structure of the fusion protein GFP-Id-HA is shown as a ribbon diagram. (C) ICAM-1 expression in HeLa cells was detected by confocal microscopy with GFP-Id-HA and mAb LB-2 staining (scale bar, 20 μm). (D) bEnd.3 cells were treated with LPS for 24 h and labeled with Id-HA conjugated to AF488 to assess cross-reactivity of human LFA-1 I domain with murine ICAM-1 (scale bar, 50 μm). (E) GFP-Id-HA was used to detect upregulated expression of ICAM-1 in LPS-treated HMEC-1 and THP-1 cells. The data are presented as the average values of fluorescence intensity (F.I.) with error bars indicating S.D. (*$p < 0.05$, unpaired Student's *t*-test compared to control group, $n = 4$).

Please cite this article in press as: Kang S, et al., Tunable physiologic interactions of adhesion molecules for inflamed cell-selective drug delivery, Biomaterials (2011), doi:10.1016/j.biomaterials.2011.01.046

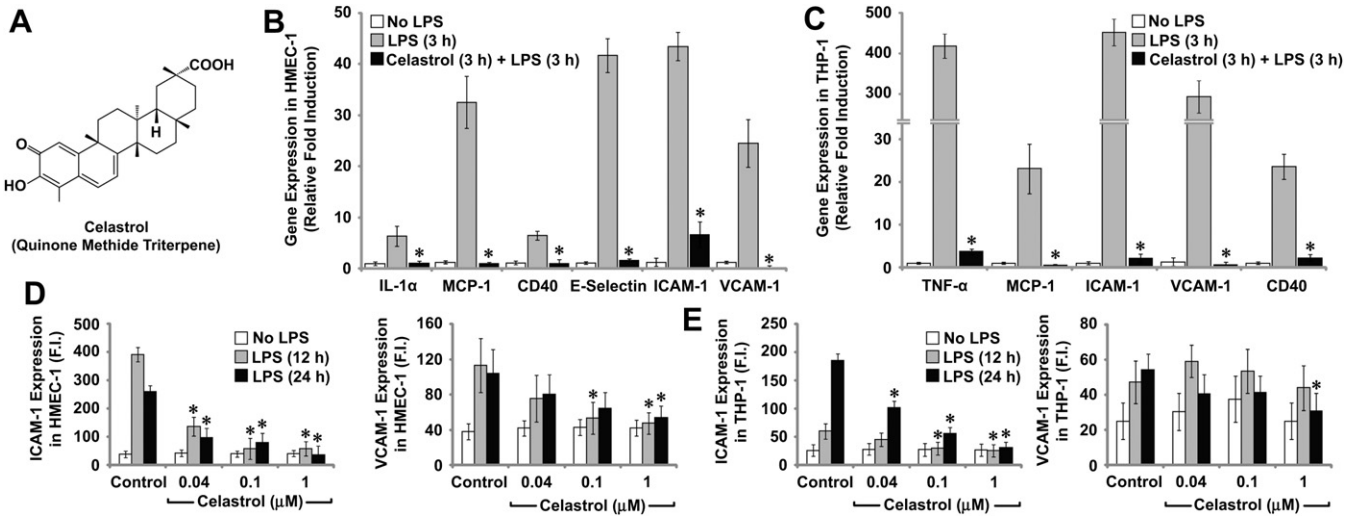

Fig. 2. Reversal of pro-inflammatory markers by celastrol in HMEC-1 and THP-1 cells. (A) The chemical structure of celastrol. (B&C) Quantitative RT-PCR was performed to measure various LPS-induced pro-inflammatory gene expression. HMEC-1 (B) and THP-1 cells (C), pretreated either with or without 1 μM celastrol for 3 h, were challenged with LPS (1 μg/ml) for 3 h before gene expression analysis. (D&E) Protein expression of cell adhesion molecules ICAM-1 (mAb LB-2) and VCAM-1 (mAb P3C4) was evaluated by flow cytometry. HMEC-1 (D) or THP-1 (E) cells were pretreated with 0.04–1 μM celastrol for 3 h and challenged with LPS (1 μg/ml) for 12 or 24 h to assess inhibition of ICAM-1 and VCAM-1 expression. The data represent the average values of fluorescent intensity (F.I.) (*$p < 0.05$, unpaired Student's *t*-test compared to the LPS group (B&C) or to control group (D&E), $n = 4$).

VCAM-1 were much larger for THP-1 cells than HMEC-1 (Fig. 2B and C), partly due to their lower levels in THP-1 at a resting state. Pretreatment with celastrol at 1 μM for 3 h, however, potently blocked LPS-induced expression of pro-inflammatory markers in both HMEC-1 and THP-1 cells (Fig. 2B and C). To examine if the suppression of pro-inflammatory markers at the mRNA level would reduce cell surface expression of cell adhesion molecules, which in effect would form a critical barrier to cell–cell adhesion and monocyte migration, we measured ICAM-1 and VCAM-1 expression by flow cytometry (Fig. 2D and E). Pretreatment of HMEC-1 with celastrol for 3 h significantly inhibited both ICAM-1 and VCAM-1 expression in a dose-dependent manner, restoring to their basal levels with 100 nM of celastrol (Fig. 2D). In THP-1 cells, a similar trend was observed, resulting in nearly complete inhibition of ICAM-1 expression with as low as 100 nM celastrol (Fig. 2E). In contrast to as much as 10-fold increase in fluorescence intensity measured for ICAM-1 in both cell lines, VCAM-1 expression was less prominent with only 3-fold induction (Fig. 2D and E). Also, inhibition of VCAM-1 expression in THP-1 cells was less potent as significant reduction was detected only with 1 μM celastrol (Fig. 2E).

3.3. Ni-NTA liposome as a drug carrier with tunable assembly with targeting moieties

Ni-NTA phospholipids (10 mol % DOGS-NTA(Ni)) were included in pegylated liposomes to assemble with polyhistidine (6 x HIS) tagged moieties, which would enable coupling of liposome nanoparticles with LFA-1 I domain variants at a predefined coating density and in a correct orientation. Unilamellar vesicles encapsulating desired drug or dye molecules were formulated by the hydration of thin lipid film in drug/dye-containing solutions, followed by the sonication and extrusion method (Fig. 3A). Liposomes encapsulating FITC or celastrol (denoted as liposome(FITC) and liposome(celastrol)) were separated from free molecules by gel filtration chromatography using size exclusion column (Fig. 3A and B), where small molecules such as FITC and celastrol eluted much later than nanoparticles (Fig. 3B). Liposomes were then mixed with Id-HA and subjected to centrifugation through a gradient of sucrose (20–30%, w/v), where Id-HA coated liposomes would float to the top of the gradient and unconjugated Id-HA remain at the bottom of the tube. The top fractions of the sucrose gradient were collected and measured for protein concentrations. Only when both liposomes and Id-HA were premixed, proteins were present at the top fractions (Fig. 3C). The size of liposomes before or after assembly with Id-HA was measured by dynamic light scattering (DLS). The diameter of the liposomes before protein conjugation was ~107 nm, which increased to ~115 nm after coupling with Id-HA, corresponding closely to a single layer of I domain ~4 nm in size. Encapsulation efficiencies (weight of drug/weight of phospholipid) of celastrol and FITC were estimated to be 0.8% and 1.5%, respectively (Fig. 3D).

3.4. Specific targeting of inflamed cells by tunable affinity and avidity of I domain and ICAM-1 interactions

Structurally and functionally homologous I domains from two different β_2 integrins, LFA-1 ($\alpha_L\beta_2$) and Mac-1 ($\alpha_M\beta_2$), both interact with ICAM-1 [25,38]. A number of mutations have been isolated to increase their binding affinity to ICAM-1, mimicking activation signals transmitted to the I domain by the neighboring domains in full-length integrins [28,35]. To test the specificities of LFA-1 and Mac-1 I domains, they were expressed on yeast cell surface in their wild-type (WT) or with activating mutations (F265S/F292G for LFA-1 [28] and F302L for Mac-1 [35]). Yeast cells expressing the WT of LFA-1 or Mac-1 I domains failed to bind strongly to HMEC-1 cells even after LPS-induced ICAM-1 expression (Fig. 4A). While the binding of yeast cells expressing LFA-1 Id-HA was specific to LPS-treated HMEC-1, yeast cells expressing Mac-1 Id-HA bound to both resting and LPS-treated HMEC-1. This indicates the presence of other ligands to Mac-1 such as fibrinogen, heparin, and ICAM-2 [38,39], which may be constitutively expressed and not dependent on LPS-induced inflammation.

We then examined whether the affinity and avidity could be fine-tuned for inflamed cell-specific targeted delivery of liposomes (Fig. 4B and C). Liposome(FITC) assembled with LFA-1 I domain variants (Id-WT, Id-HA, or Id-D137A) or without a targeting moiety were incubated with LPS-treated HMEC-1 (Fig. 4B). The mutation D137A abolishes the metal ion coordination in the MIDAS and inactivates I domain binding to ligands [40]. The maximum delivery

Please cite this article in press as: Kang S, et al., Tunable physiologic interactions of adhesion molecules for inflamed cell-selective drug delivery, Biomaterials (2011), doi:10.1016/j.biomaterials.2011.01.046

of liposome(FITC) was observed when coupled with Id-HA, whereas much lower binding was achieved with Id-WT (Fig. 4B). As expected, liposomes coated with Id-D137A or without a moiety did not bind to LPS-treated HMEC-1 cells. To examine the avidity effect of interactions between the Id-HA and ICAM-1 on the efficiency of liposome delivery and specificity to inflamed cells, liposome nanoparticles were coupled with a varying amounts of Id-HA in the range of 10–40% mass ratio (w/w) of protein to phospholipid

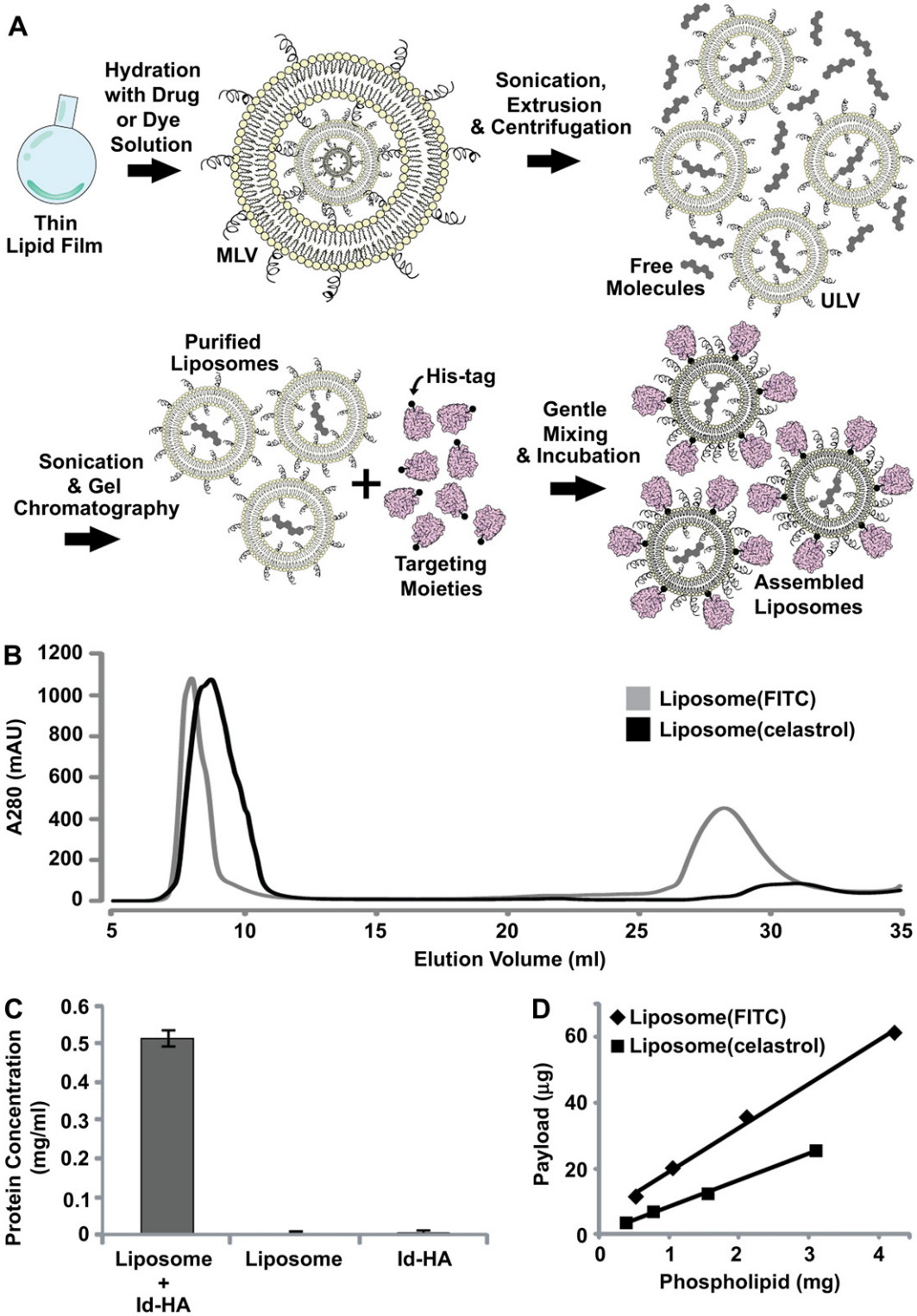

Fig. 3. Ni-NTA liposome for spontaneous assembly with the I domains. (A) The schematic depicts the process of formulating targeted liposome, highlighting the steps of thin lipid film hydration, extrusion of multilamellar vesicles (MLV) to unilamellar vesicles (ULV), payload encapsulation, purification, and spontaneous assembly with His-tagged targeting moieties. (B) The elution profiles of FITC or celastrol containing liposome from S200 size exclusion column are shown. (C) The amount of proteins assembled with Ni-NTA liposome was measured from the top fractions after sucrose gradient flotation assay. (D) Encapsulation efficiencies of FITC (1.5%) and celastrol (0.8%) were measured from the weight ratio of the payload to phospholipids.

Please cite this article in press as: Kang S, et al., Tunable physiologic interactions of adhesion molecules for inflamed cell-selective drug delivery, Biomaterials (2011), doi:10.1016/j.biomaterials.2011.01.046

(Fig. 4C). Liposomes coated with ~40% (w/w) Id-HA showed a highest level of delivery to active HMEC-1, which was also associated with significant binding to resting HMEC-1. At 20% Id-HA, although the level of binding to LPS-treated HMEC-1 was reduced, liposome delivery to resting HMEC-1 was not detectable. When the mass ratio of Id-HA to phospholipids was further reduced to 10%, liposome delivery to LPS-treated HMEC-1 was only faintly detectable. These results highlight the importance of the ability to fine-

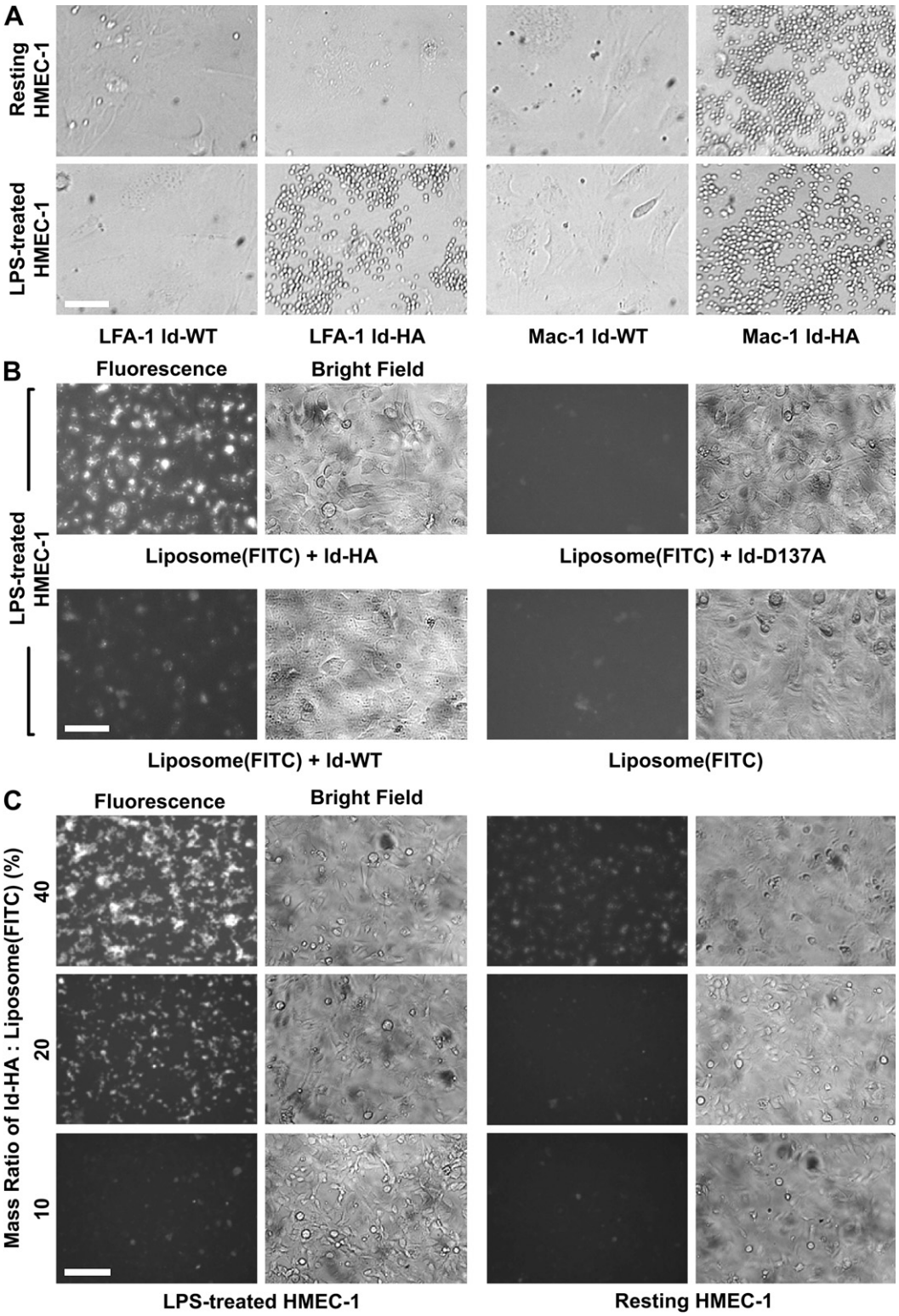

Fig. 4. Targeted delivery by tunable affinity and avidity of targeting moieties on liposomes. (A) The wild-type or the active I domains of LFA-1 or Mac-1 integrins displayed on yeast cells were examined for binding to either resting or LPS-treated HMEC-1 (scale bar, 50 μm). (B) Microscopic fluorescence images of LPS-treated HMEC-1 after 30 min incubation with nanoparticles assembled with LFA-1 I domain variants (Id-WT, Id-HA, and Id-D137A) or without a targeting moiety are shown (scale bar, 50 μm). (C) Liposome(FITC) assembled with mass ratios of Id-HA to phospholipids ranging from 10 to 40% were incubated with LPS-treated HMEC-1 for 30 min to fine-tune avidity interaction to overexpressed ICAM-1 (scale bar, 100 μm).

Please cite this article in press as: Kang S, et al., Tunable physiologic interactions of adhesion molecules for inflamed cell-selective drug delivery, Biomaterials (2011), doi:10.1016/j.biomaterials.2011.01.046

tune both affinity and avidity of targeting moieties in delivering nanoparticles to differentially expressed endogenous cell surface molecules.

3.5. Optimal concentration of celastrol that is anti-inflammatory but not cytotoxic

In order to find an optimal dosage of celastrol that effectively elicits therapeutic efficacy with minimum cytotoxicity, we examined dose-dependent suppression of pro-inflammatory markers and cell viability of HMEC-1. To better mimic *in vivo* condition where the target cells may be exposed to nanoparticles for a relatively short time due to the clearance of nanoparticles from the body, 30 min incubation with celastrol or liposome(celastrol) was applied to LPS-treated HMEC-1 or THP-1 cells (Fig. 5). Celastrol began to show a dose-dependent inhibitory effect on gene expression of VCAM-1, ICAM-1, and MCP-1 with as low as 10 nM concentration, with a steady increase in inhibition with an increase in drug dose (Fig. 5A and B). We then evaluated the corresponding cell viability of LPS-treated HMEC-1 after treatment with celastrol at various concentrations (Fig. 5C). Cell viability was significantly reduced starting with 10 μM celastrol treatment for 30 min. Treatment with 1 μM celastrol, however, did not produce any significant cytotoxic effect (Fig. 5C). We also evaluated the cytotoxicity of liposome containing 1 μM celastrol. Liposome(celastrol) coupled with ~20% (w/w) Id-HA or without a targeting moiety did not produce significant cell death in HMEC-1 for (Fig. 5C).

3.6. Suppression of pro-inflammatory gene expression by targeted delivery of celastrol

A mass ratio of ~20% Id-HA to phospholipid and a dosage of celastrol at ~1 μM were chosen for the specificity towards inflamed cells and for the lack of cytotoxicity. With these conditions, we examined the inhibitory effect of targeted delivery of liposome (celastrol) on pro-inflammatory marker expression in HMEC-1 and THP-1 cells. To simulate the reinitiating loop of inflammatory signals in the milieu of endothelium/immune cells and to examine the efficacy of targeted delivery on inhibition of inflammation therein, both HMEC-1 and THP-1 cells were first treated with LPS for 24 h before liposome(celastrol) delivery (Fig. 6A). At 36–48 h after 30 min treatment of liposome(celastrol), cells were then challenged with LPS for another 3 h, followed by gene expression analysis (Fig. 6A). In both HMEC-1 and THP-1 cells, targeted delivery of liposome(celastrol) was as effective or superior to the same dosage of free celastrol (Fig. 6B). The inhibitory effect of liposome(celastrol) in HMEC-1 cells was dependent on specific molecular interaction with ICAM-1, evidenced by the lack of inhibition when coupled with

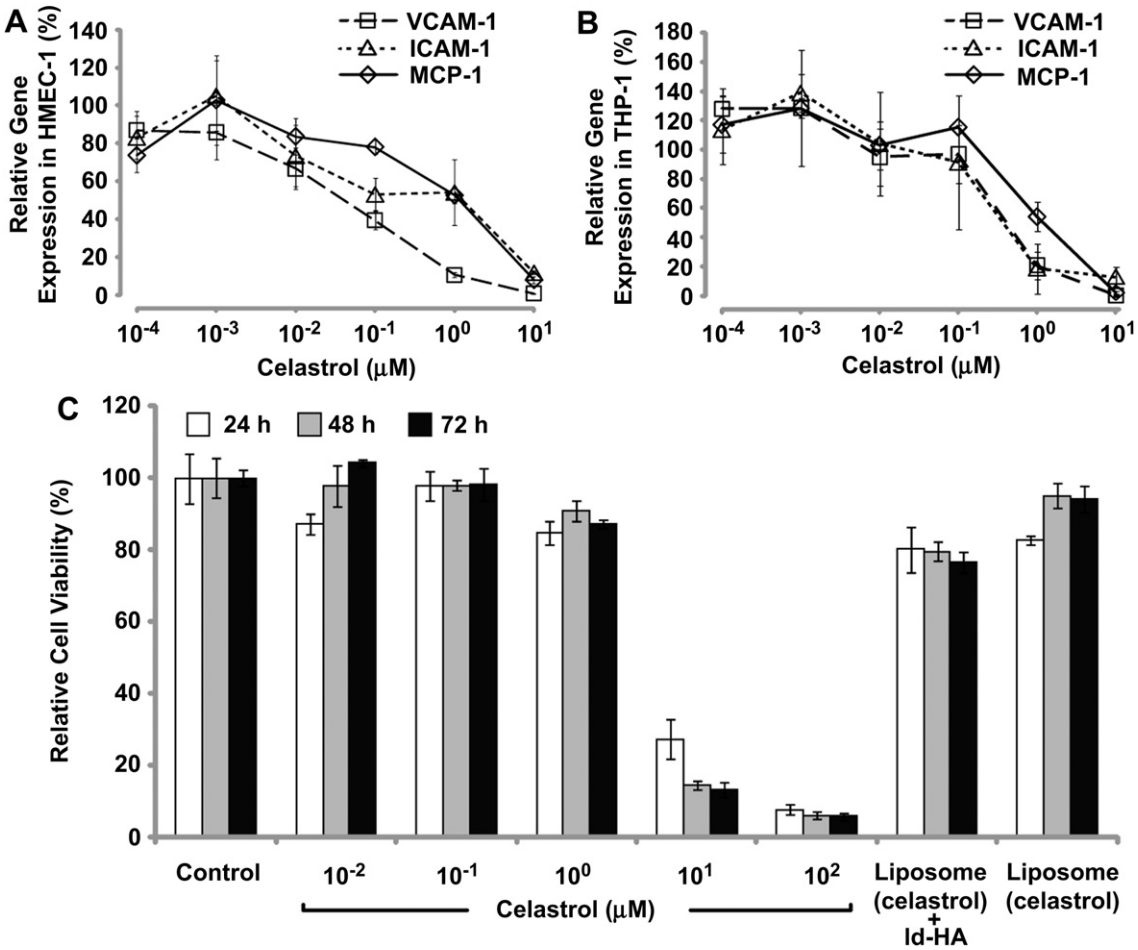

Fig. 5. Optimal dosage of celastrol that is anti-inflammatory but not cytotoxic. (A&B) Dose-dependent anti-inflammatory effect of celastrol was evaluated by qPCR analysis for LPS-induced pro-inflammatory gene expression. HMEC-1 (A) and THP-1 cells (B) were incubated with celastrol (100 pM–10 μM for 30 min), challenged with LPS (1 μg/ml, 3 h) 36 h after celastrol treatment, and examined for inhibition of gene expression of VCAM-1, ICAM-1, and MCP-1. Data are presented as the percentage of gene expression relative to LPS-treated, no celastrol control groups ($n = 4$). (C) The effect of celastrol treatment on cell viability of LPS-treated HMEC-1 was evaluated at 72 h. Liposome containing ~1 μM celastrol assembled with or without Id-HA was also evaluated for cell viability ($n = 4$).

Please cite this article in press as: Kang S, et al., Tunable physiologic interactions of adhesion molecules for inflamed cell-selective drug delivery, Biomaterials (2011), doi:10.1016/j.biomaterials.2011.01.046

Id-D137A (Fig. 6B). In THP-1 cells, a maximum inhibition of pro-inflammatory marker expression was seen with liposome(celastrol) coated with Id-HA, although some level of inhibition was also observed with non-targeted delivery with Id-D173A (Fig. 6B). This may be attributed to the non-specific uptake of liposomes by THP-1 cells that differentiate into macrophage-like phenotype upon inflammatory stimuli, exhibiting phagocytic activities independent of molecular interactions [41].

3.7. Potent inhibition of monocyte adhesion to the endothelium by targeted delivery of celastrol

Inhibition of the continuing accumulation of immune cells to inflamed vasculature will be an important measure that anti-inflammatory therapies should demonstrate. As a functional assay to measure the efficacy of targeted delivery of liposome(celastrol), we examined the attenuation of cell surface expression of ICAM-1 and the inhibition of THP-1 cell adhesion to HMEC-1. Similarly as before, HMEC-1 were treated with LPS for 24 h before liposome (celastrol) delivery, followed by a second LPS challenge 36–48 h after the delivery (Fig. 7A). The measurements of ICAM-1 expression and THP-1 adhesion were performed 24 h after the second LPS challenge to allow sufficient time for cells to respond at the protein level (Fig. 7A). The amount of ICAM-1 expression measured by mAb LB-2 was significantly lower with the targeted delivery of liposome (celastrol) coupled with Id-HA than free celastrol (Fig. 7B). Liposome(celastrol) coupled with Id-D137A produced little suppression of ICAM-1 expression compared with free celastrol, implying a minimum non-specific uptake of liposomes by HMEC-1 and a minimum escape of encapsulated celastrol from the liposomes (Fig. 7B). LPS-induced proliferation [42] of HMEC-1 was also significantly inhibited by targeted delivery of liposome(celastrol)

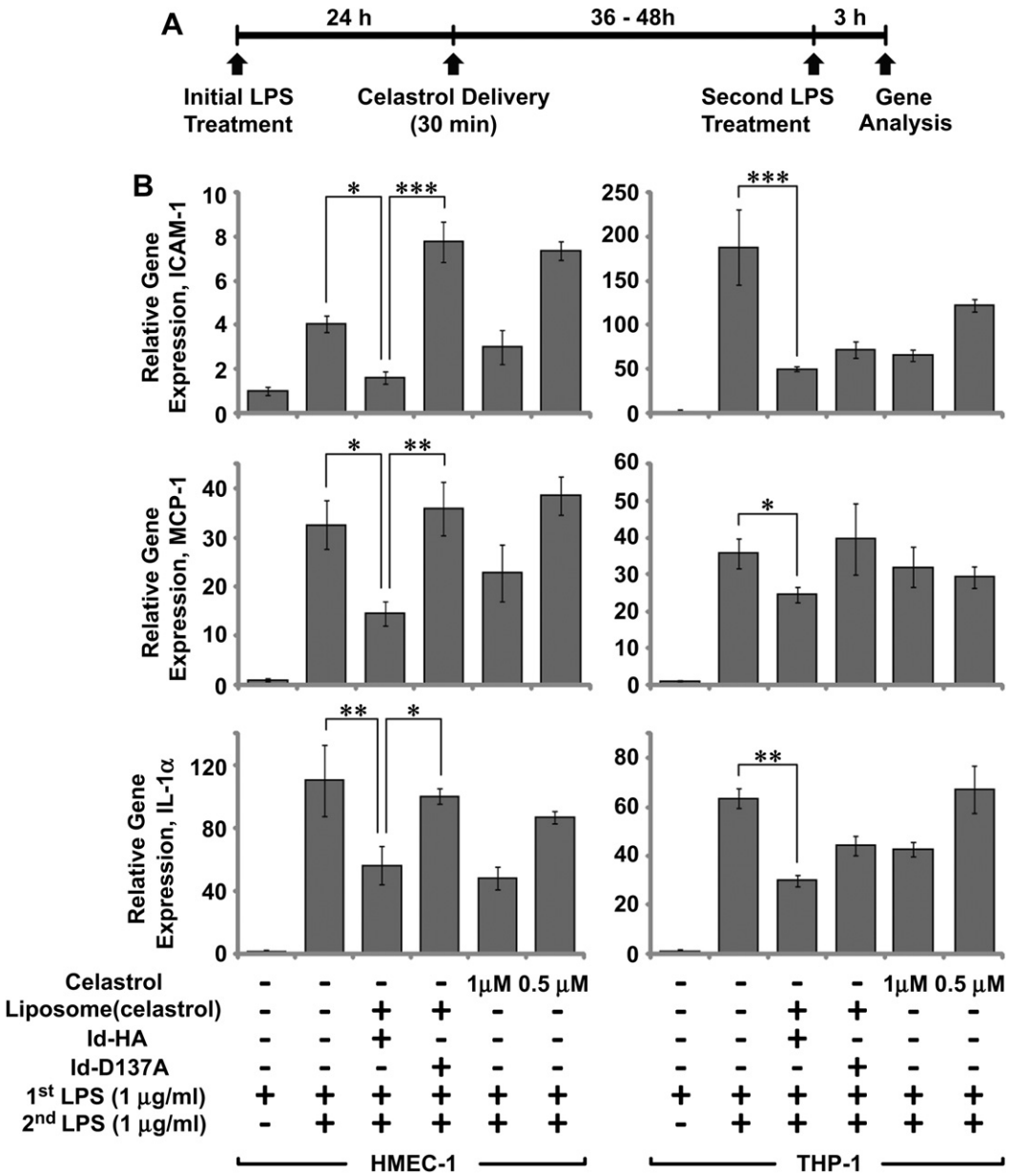

Fig. 6. Suppression of pro-inflammatory gene expression by targeted delivery of celastrol. (A) The timeline shows the sequence of the treatment with LPS, celastrol delivery, and gene analysis by qPCR. (B) Gene expression of ICAM-1, MCP-1, and IL-1α was examined to assess therapeutic efficacy of targeted delivery of celastrol. Liposome containing ~1 μM celastrol coupled with Id-HA or Id-D137A or free celastrol at 0.5 or 1 μM were delivered to HMEC-1 and THP-1 cells (one-way ANOVA followed by Tukey's post-hoc test, $*p < 0.05$, $**p < 0.01$, and $***p < 0.001$, $n = 4$).

Please cite this article in press as: Kang S, et al., Tunable physiologic interactions of adhesion molecules for inflamed cell-selective drug delivery, Biomaterials (2011), doi:10.1016/j.biomaterials.2011.01.046

evidenced by cell density (Fig. 7C). However, free celastrol of equal concentration did not exhibit the anti-proliferative effect of the drug and failed to inhibit endothelial proliferation followed by LPS injury (Fig. 7C). The levels of ICAM-1 suppression on HMEC-1 surface also led to a proportional decrease in the adhesion of THP-1 cells to HMEC-1, i.e., a maximum inhibition seen with Id-HA coated liposome(celastrol) followed by free celastrol, while no change was observed with Id-D137A coated liposomes (Fig. 7D and E). Enhanced inhibition of ICAM-1 expression and THP-1 cell adhesion by Id-HA coated liposome(celastrol) as compared with free celastrol may be due to more potent suppression of ICAM-1 gene expression (Fig. 6B) and reduction of ICAM-1 surface density (Fig. 7B) impelled by the binding and subsequent internalization of Id-HA coated liposome(celastrol).

4. Discussion

Comprehensive inflamed cell-specific targeted delivery may contribute to a more effective clinical use of potent anti-inflammatory drugs against a broad spectrum of immune and inflammatory diseases. The challenge of targeting overexpressed endogenous molecules for selective delivery is that these molecules may also be present in cells outside of the disease sites. In addition, diverse cellular players that together form reciprocal inflammatory signals pose another challenge to delivery strategies targeting only either immune or non-immune cells. Thus ensuring specificity as well as the spectrum of cellular components that drug carriers can influence should be considered as two important factors for an effective treatment for immune and inflammatory diseases. In this study, we investigated a strategy to address both issues of specificity and comprehensive targeting by the choice of ICAM-1, which is greatly upregulated broadly over both non-immune and immune cells under inflammation, and exploiting its physiological interaction with LFA-1 integrin for inflamed cell-specific delivery of anti-inflammatory agents. This design criteria led us to use liposomal nanoparticles coated at a tunable density with the LFA-1 I domain, of which a collection of engineered variants are available for differing affinity to ICAM-1 in the range of mM to nM K_D [28]. Our ICAM-1 targeting strategy, therefore, mimics to a great extent an intrinsic behavior of leukocytes that bind selectively to the inflammatory sites by modulating affinity and avidity of integrins [43] for targeting inflammation.

Preferential and comprehensive delivery of celastrol, a potent anti-inflammatory, anti-oxidative, and anti-proliferative drug [32–34], was demonstrated against the cell lines of endothelium (HMEC-1) and monocytes/macrophages (THP-1), which displayed dramatic upregulation of ICAM-1 after LPS challenge. Unlike soluble monomeric molecule binding to ICAM-1, multivalent interactions will be required for effective binding of nanoparticles of ~100 nm in diameter to resist thermal diffusion and detachment force exerted by fluid-induced shear stress. This is to some extent analogous to the binding and the entry of human rhinoviruses (a non-enveloped viral

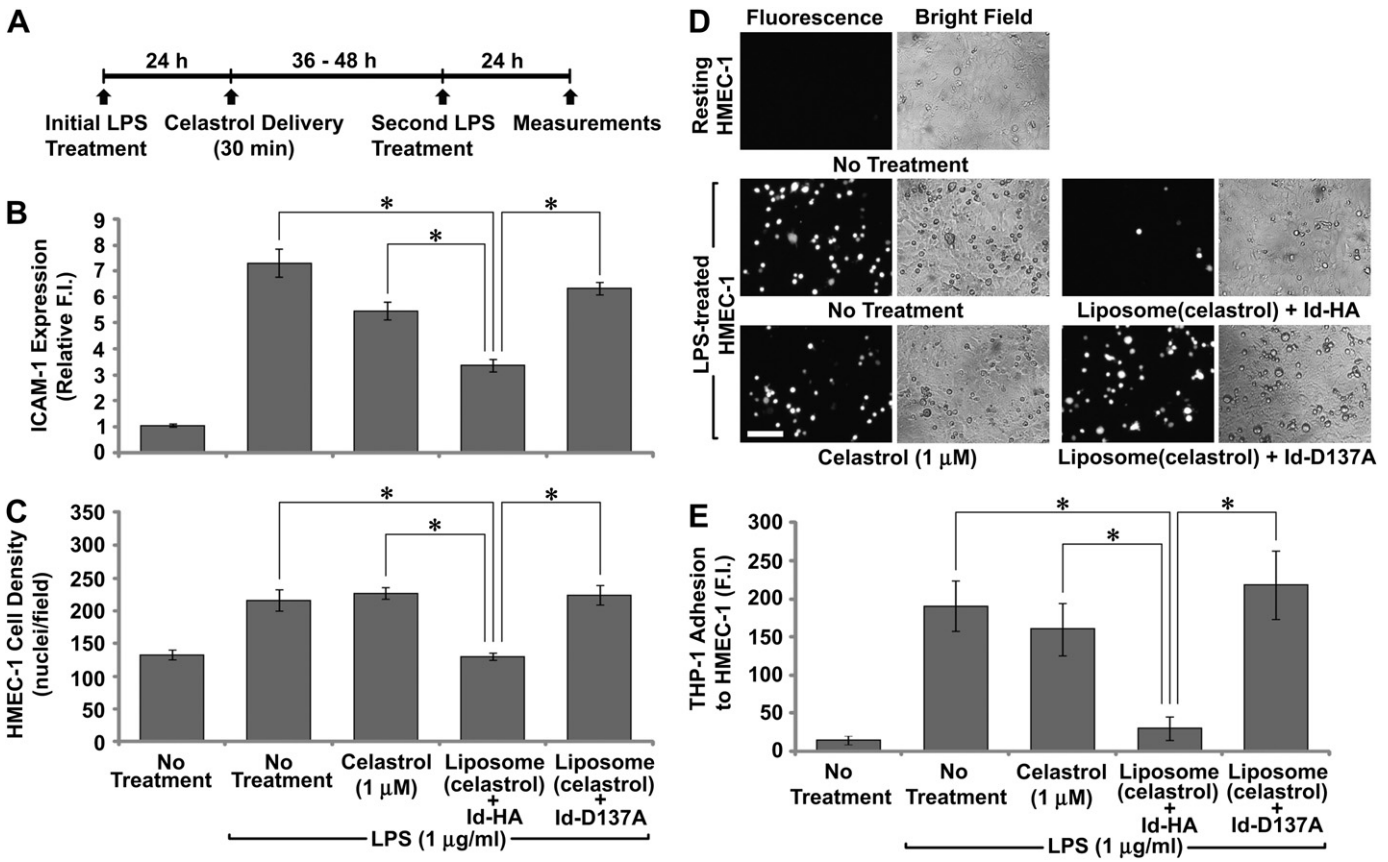

Fig. 7. Potent inhibition of HMEC-1 proliferation and THP-1 adhesion by targeted delivery of celastrol. (A) The timeline shows the sequence of the treatment with LPS, celastrol delivery, and the measurements of anti-inflammatory effect at the protein level and immune cell accumulation. (B) The amount of ICAM-1 expression in HMEC-1 after targeted delivery of liposome (celastrol) was assessed by staining with mAb LB-2 ($^*p < 0.001$, $n = 4$). (C) The effect of targeted delivery of liposome (celastrol) was also tested for its ability to inhibit LPS-induced proliferation of HMEC-1 or increase in cell density, estimated by the number of nuclei (identified with DAPI) per microscopic field (1.5 x 10^5 μm^2) ($^*p < 0.001$, $n = 4$). (D) Representative microscopic fluorescence images show BCECF-labeled THP-1 cell adhesion to LPS-treated HMEC-1 after delivery of celastrol (scale bar, 100 μm). (E) Fluorescence of whole lysates of adhered BCECF-labeled THP-1 cells was measured ($^*p < 0.001$, $n = 6$). (B, C,&E) One-way ANOVA followed by Tukey's post-hoc test was performed to obtain statistical significance.

Please cite this article in press as: Kang S, et al., Tunable physiologic interactions of adhesion molecules for inflamed cell-selective drug delivery, Biomaterials (2011), doi:10.1016/j.biomaterials.2011.01.046

particle with ~35 nm diameter capsid), which shows little binding to cells with basal levels of ICAM-1 expression, but becomes rapidly internalized into cells after upregulated expression of ICAM-1 by cytokines or other pro-inflammatory agents [44]. The requirement for multivalency interaction was supported by the observation that a higher coating density of the I domain on FITC-containing liposomes led to an increase in fluorescence intensity in HMEC-1. At the highest coating density of I domain, a low level of fluorescence began to show up even in resting HMEC-1 without LPS challenge. Previously, we have reported a correlation between the intrinsic affinity of the I domain (due to different mutations) to ICAM-1 and the efficiency of nanoparticle delivery into ICAM-1 overexpressing tumor cells [30]. In the current study, we used either the wild-type or active I domain containing F265S/F292G and varied the coating density of the I domains to ensure selective delivery against inflamed cells. The versatility of our ICAM-1 targeting strategy by virtue of affinity and avidity modulation is absent in most previous approaches based on monoclonal antibodies or short peptides with largely uncharacterized affinities to ICAM-1. Also, chemical conjugation methods were used to attach targeting moieties to nanoparticles, which unavoidably resulted in aggregation and uncertainty in the number of functional molecules per particle. The ability to fine-tune the avidity by simple mixing of the I domains and liposomes at varying ratios as well as the affinity by the use of different I domain variants (e.g., F292A (K_D ~10 mM), F292G (K_D ~100 nM), and F265S/F292G (K_D ~6 nM)) will likely be more critical for *in vivo* studies, which would involve different disease types or severity of inflammation and ICAM-1 expression, and different rheology and hemodynamic forces in arteries versus peripheral blood vessels.

The inhibitory effect on pro-inflammatory gene expression by targeted delivery *in vitro* was in general more effective than free celastrol at equal dosage. Non-specific uptake of free celastrol or many other small molecule compounds in this matter will probably be due to the hydrophobic nature of the compounds, which would aggregate in aqueous solution and be taken up by cells [45]. In contrast, the inhibitory effect of celastrol encapsulated in liposome was dependent on the specific molecular interactions of ICAM-1 with Id-HA, evidenced by the lack of inhibition with Id-D137A coated liposome. *In vivo* benefit and efficacy of selective delivery of anti-inflammatory drugs via liposomes will more likely be pronounced in a clinical perspective, considering many problems associated with parenteral administration of hydrophobic and poorly water-soluble drugs such as low absorption and bioavailability, and side effects due to non-selective, systemic cytotoxicity. Furthermore, targeted delivery to ICAM-1 may not only directly compete with ICAM-1 specific cell adhesion molecules for immune cell adhesion to inflamed vascular endothelium but also reduce surface density of ICAM-1 by causing multivalent clustering and subsequent internalization of ICAM-1 [46]. Such potent inhibition of immune cell accumulation, inflamed cell-selective intracellular delivery of the drug, and alleviation of pro-inflammatory signals *in vivo* for the treatment of acute and chronic inflammatory diseases would be difficult to achieve with free celastrol. Moreover, considering anti-proliferative and cytotoxic effects at higher dosage of celastrol, applications of ICAM-1 directed delivery may be extended to neovasculatures in tumors and proliferative immune cells in atherosclerotic lesions without significant adverse systemic side effects.

Cell surface molecules that are induced under inflammation and therefore have been used for targeted delivery of imaging agents and drugs include E- and P-selectins, ICAM-1, and VCAM-1. Although VCAM-1 has been more frequently chosen as a marker for inflamed vasculature, our studies clearly show several advantages of targeting ICAM-1 due to its higher degree of induction in both non-immune and immune cells, rendering an opportunity to deliver anti-inflammatory agents to the greater part of the cellular culprits in inflammatory diseases. Such properties of ICAM-1 greatly supports the use of the physiologic counter-receptors to ICAM-1 for inflamed cell-specific targeted drug delivery. Among the major integrin receptors against ICAM-1 such as LFA-1 and Mac-1, we found that active Mac-1 I domain exhibited binding to resting endothelium, indicating the presence of high affinity inflammation-independent ligands for Mac-1. Despite the fact that quiescent HMEC-1 constitutively expresses other physiologic ligands of LFA-1 such as ICAM-2 [47], inflammation-specific delivery of Id-HA coated liposomes is consistent with the observation that LFA-1 integrin has at least 10-fold higher affinity to ICAM-1 than to other ICAM members. Another cell adhesion molecule called junctional adhesion molecule (JAM)-1 redistributes from cell junctions to the accessible apical surface of endothelial cells under inflammation, which may also contribute to adhesion and transmigration of leukocytes through its putative interaction with LFA-1 [48]. Although little is known in regard to the affinity of LFA-1 to JAM-1 and if the I domain variants engineered for high affinity to ICAM-1 would also bind better to JAM-1, the use of LFA-1 I domain may be extended to targeting JAM-1 to potentiate inflammation-specific delivery.

In summary, our study demonstrates the importance of specificity, affinity, and avidity of targeting moieties on nanoparticles as important design parameters for selective drug carriers. Specific delivery of nanoparticle carriers should therefore optimize molecular interactions from all these perspectives, rather than focusing only on monomeric affinity between two interacting, soluble molecules. The optimization of molecular interactions can be facilitated greatly with tunable physiologic interactions such as those in LFA-1 I domain and ICAM-1 in this study, resulting in preferential to specific binding of nanoparticles to inflamed HMEC-1 and THP-1 cells with little delivery into resting cells. Targeting ICAM-1 via its interaction with LFA-1 I domain would thus be of a great clinical use for inflamed cell-specific targeted delivery and may contribute for safer and more comprehensive treatments with anti-inflammatory agents against a broad range of immune and inflammatory diseases.

5. Conclusion

Dysregulated inflammatory responses of host immune system contributes to the pathogenesis of various human diseases. Clinical use of anti-inflammatory agents to treat resilient immune and inflammatory diseases, however, have met with limited success, attributable to insufficient dosage of drugs to diseased sites and adverse systemic side effects. In order to achieve selective drug delivery into inflamed sites, we have developed liposomal nanoparticles encapsulating anti-inflammatory drugs and coated with targeting moieties against ICAM-1, a cell adhesion molecule greatly upregulated both in inflamed immune and vascular cells. Using a physiological ligand called LFA-1 I domain, we demonstrate that the ability to fine-tune affinity and avidity with target receptor on cells is critical to the design of inflammation targeting drug carriers to ensure specificity and to avoid toxicities. The utility of physiological interactions for selective drug carriers can be extended to treating a broad spectrum of immune and inflammatory disease.

Acknowledgements

This work was supported by a Scientist Development Grant (M.M.J.) and a Predoctoral Fellowship (S.K.) offered by American Heart Association. We thank the assistance of Carol J. Bayles and the Microscopy and Imaging Facility of the Cornell Biotechnology Research Center.

Please cite this article in press as: Kang S, et al., Tunable physiologic interactions of adhesion molecules for inflamed cell-selective drug delivery, Biomaterials (2011), doi:10.1016/j.biomaterials.2011.01.046

Appendix

Figures with essential color discrimination. Fig. 3 in this article are difficult to interpret in black and white. The full color images can be found in the online version, at doi:10.1016/j.biomaterials.2011.01.046.

References

[1] Nathan C, Ding A. Nonresolving inflammation. Cell 2010;140(6):871–82.
[2] Libby P. Inflammation in atherosclerosis. Nature 2002;420(6917):868–74.
[3] Hotamisligil GS. Inflammation and metabolic disorders. Nature 2006; 444(7121):860–7.
[4] Glass CK, Saijo K, Winner B, Marchetto MC, Gage FH. Mechanisms underlying inflammation in neurodegeneration. Cell 2010;140(6):918–34.
[5] Coussens LM, Werb Z. Inflammation and cancer. Nature 2002;420(6917): 860–7.
[6] FitzGerald GA, Patrono C. The coxibs, selective inhibitors of cyclooxygenase-2. N Engl J Med 2001;345(6):433–42.
[7] Jain MK, Ridker PM. Anti-inflammatory effects of statins: clinical evidence and basic mechanisms. Nat Rev Drug Discov 2005;4(12):977–87.
[8] Patrono C, Garcia Rodriguez LA, Landolfi R, Baigent C. Low-dose aspirin for the prevention of atherothrombosis. N Engl J Med 2005;353(22):2373–83.
[9] Rhen T, Cidlowski JA. Antiinflammatory action of glucocorticoids–new mechanisms for old drugs. N Engl J Med 2005;353(16):1711–23.
[10] Ridker PM, Cushman M, Stampfer MJ, Tracy RP, Hennekens CH. Inflammation, aspirin, and the risk of cardiovascular disease in apparently healthy men. N Engl J Med 1997;336(14):973–9.
[11] Schacke H, Docke WD, Asadullah K. Mechanisms involved in the side effects of glucocorticoids. Pharmacol Ther 2002;96(1):23–43.
[12] Fitzgerald GA. Coxibs and cardiovascular disease. N Engl J Med 2004; 351(17):1709–11.
[13] Hanai J, Cao P, Tanksale P, Imamura S, Koshimizu E, Zhao J, et al. The muscle-specific ubiquitin ligase atrogin-1/MAFbx mediates statin-induced muscle toxicity. J Clin Invest 2007;117(12):3940–51.
[14] Allen TM, Cullis PR. Drug delivery systems: entering the mainstream. Science 2004;303(5665):1818–22.
[15] Muzykantov VR. Targeting of superoxide dismutase and catalase to vascular endothelium. J Control Release 2001;71(1):1–21.
[16] Muro S, Dziubla T, Qiu WN, Leferovich J, Cui X, Berk E, et al. Endothelial targeting of high-affinity multivalent polymer nanocarriers directed to intercellular adhesion molecule 1. J Pharmacol Exp Ther 2006;317(3): 1161–9.
[17] Kelly KA, Allport JR, Tsourkas A, Shinde-Patil VR, Josephson L, Weissleder R. Detection of vascular adhesion molecule-1 expression using a novel multimodal nanoparticle. Circ Res 2005;96(3):327–36.
[18] Voinea M, Manduteanu I, Dragomir E, Capraru M, Simionescu M. Immunoliposomes directed toward VCAM-1 interact specifically with activated endothelial cells–a potential tool for specific drug delivery. Pharm Res 2005; 22(11):1906–17.
[19] Kozower BD, Christofidou-Solomidou M, Sweitzer TD, Muro S, Buerk DG, Solomides CC, et al. Immunotargeting of catalase to the pulmonary endothelium alleviates oxidative stress and reduces acute lung transplantation injury. Nat Biotechnol 2003;21(4):392–8.
[20] Spragg DD, Alford DR, Greferath R, Larsen CE, Lee KD, Gurtner GC, et al. Immunotargeting of liposomes to activated vascular endothelial cells: a strategy for site-selective delivery in the cardiovascular system. Proc Natl Acad Sci USA 1997;94(16):8795–800.
[21] Ehrhardt C, Kneuer C, Bakowsky U. Selectins-an emerging target for drug delivery. Adv Drug Deliv Rev 2004;56(4):527–49.
[22] Arap W, Pasqualini R, Ruoslahti E. Cancer treatment by targeted drug delivery to tumor vasculature in a mouse model. Science 1998;279(5349):377–80.
[23] Sugahara KN, Teesalu T, Karmali PP, Kotamraju VR, Agemy L, Girard OM, et al. Tissue-penetrating delivery of compounds and nanoparticles into tumors. Cancer Cell 2009;16(6):510–20.
[24] Dustin ML, Rothlein R, Bhan AK, Dinarello CA, Springer TA. Induction by IL 1 and interferon-gamma: tissue distribution, biochemistry, and function of a natural adherence molecule (ICAM-1). J Immunol 1986;137(1):245–54.
[25] Marlin SD, Springer TA. Purified intercellular-adhesion molecule-1 (ICAM-1) is a ligand for lymphocyte function-associated antigen-1 (LFA-1). Cell 1987; 51(5):813–9.
[26] Dunehoo AL, Anderson M, Majumdar S, Kobayashi N, Berkland C, Siahaan TJ. Cell adhesion molecules for targeted drug delivery. J Pharm Sci 2006; 95(9):1856–72.
[27] Simone E, Ding BS, Muzykantov V. Targeted delivery of therapeutics to endothelium. Cell Tissue Res 2009;335(1):283–300.
[28] Jin M, Song G, Carman CV, Kim YS, Astrof NS, Shimaoka M, et al. Directed evolution to probe protein allostery and integrin I domains of 200,000-fold higher affinity. Proc Natl Acad Sci USA 2006;103(15):5758–63.
[29] Phan UT, Waldron T, Springer TA. Remodeling of the lectin-EGF-like domain interface in P- and L-selectin increases adhesiveness and shear resistance under hydrodynamic force. Nat Immunol 2006;7(8):883–9.
[30] Park S, Kang S, Veach AJ, Vedvyas Y, Zarnegar R, Kim JY, et al. Self-assembled nanoplatform for targeted delivery of chemotherapy agents via affinity-regulated molecular interactions. Biomaterials 2010;31(30):7766–75.
[31] Almenarqueralt A, Duperray A, Miles LA, Felez J, Altieri DC. Apical topography and modulation of ICAM-1 expression on activated endothelium. Am J Pathol 1995;147(5):1278–88.
[32] Lee JH, Koo TH, Yoon H, Jung HS, Jin HZ, Lee K, et al. Inhibition of NF-kappa B activation through targeting I kappa B kinase by celastrol, a quinone methide triterpenoid. Biochem Pharmacol 2006;72(10):1311–21.
[33] Yang HJ, Chen D, Cui QZC, Yuan X, Dou QP. Celastrol, a triterpene extracted from the Chinese "Thunder of God Vine," is a potent proteasome inhibitor and suppresses human prostate cancer growth in nude mice. Cancer Res 2006;66 (9):4758–65.
[34] Mu TW, Ong DST, Wang YJ, Balch WE, Yates JR, Segatori L, et al. Chemical and biological approaches synergize to ameliorate protein-folding diseases. Cell 2008;134(5):769–81.
[35] Hu X, Kang S, Lefort C, Kim M, Jin MM. Combinatorial libraries against libraries for selecting neoepitope activation-specific antibodies. Proc Natl Acad Sci USA 2010;107(14):6252–7.
[36] Szoka F, Olson F, Heath T, Vail W, Mayhew E, Papahadjopoulos D. Preparation of unilamellar liposomes of intermediate size (0.1-0.2 mumol) by a combination of reverse phase evaporation and extrusion through polycarbonate membranes. Biochim Biophys Acta 1980;601(3):559–71.
[37] Chow JC, Young DW, Golenbock DT, Christ WJ, Gusovsky F. Toll-like receptor-4 mediates lipopolysaccharide-induced signal transduction. J Biol Chem 1999;274(16):10689–92.
[38] Diamond MS, Staunton DE, Marlin SD, Springer TA. Binding of the integrin Mac-1 (CD11b/CD18) to the third immunoglobulin-like domain of ICAM-1 (CD54) and its regulation by glycosylation. Cell 1991;65(6):961–71.
[39] Xie J, Li R, Kotovuori P, Vermot-Desroches C, Wijdenes J, Arnaout MA, et al. Intercellular adhesion molecule-2 (CD102) binds to the leukocyte integrin CD11b/CD18 through the A domain. J Immunol 1995;155(7):3619–28.
[40] Lupher ML, Harris EAS, Beals CR, Sui LM, Liddington RC, Staunton DE. Cellular activation of leukocyte function-associated antigen-1 and its affinity are regulated at the I domain allosteric site. J Immunol 2001;167(3):1431–9.
[41] Takashiba S, Van Dyke TE, Amar S, Murayama Y, Soskolne AW, Shapira L. Differentiation of monocytes to macrophages primes cells for lipopolysaccharide stimulation via accumulation of cytoplasmic nuclear factor kappa B. Infect Immun 1999;67(11):5573–8.
[42] Penn MS, Chisolm GM. Relation between lipopolysaccharide-induced endothelial-cell injury and entry of macromolecules into the rat aorta in vivo. Circ Res 1991;68(5):1259–69.
[43] Stewart M, Hogg N. Regulation of leukocyte integrin function: affinity vs avidity. J Cell Biochem 1996;61(4):554–61.
[44] Subauste MC, Jacoby DB, Richards SM, Proud D. Infection of a human respiratory epithelial-cell line with rhinovirus. Induction of cytokine release and modulation of susceptibility to infection by cytokine exposure. J Clin Invest 1995;96(1):549–57.
[45] Johnson JLH, He Y, Yalkowsky SH. Prediction of precipitation-induced phlebitis: a statistical validation of an in vitro model. J Pharm Sci 2003;92(8):1574–81.
[46] Muro S, Wiewrodt R, Thomas A, Koniaris L, Albelda SM, Muzykantov VR, et al. A novel endocytic pathway induced by clustering endothelial ICAM-1 or PECAM-1. J Cell Sci 2003;116(8):1599–609.
[47] Staunton DE, Dustin ML, Springer TA. Functional cloning of ICAM-2, a cell adhesion ligand for LFA-1 homologous to ICAM-1. Nature 1989;339(6219):61–4.
[48] Weber C, Fraemohs L, Dejana E. The role of junctional adhesion molecules in vascular inflammation. Nat Rev Immunol 2007;7(6):467–77.

Please cite this article in press as: Kang S, et al., Tunable physiologic interactions of adhesion molecules for inflamed cell-selective drug delivery, Biomaterials (2011), doi:10.1016/j.biomaterials.2011.01.046